

High proportions of regulatory B and T cells are associated with decreased cellular responses to pH1N1 influenza vaccine in HIV-infected children and youth (IMPAACT P1088)

Adriana Weinberg,^{1,*} Petronella Muresan,² Terence Fenton,³ Kelly Richardson,¹ Teresa Dominguez,¹ Anthony Bloom,⁴ Elizabeth Petzold,⁵ Patricia Anthony,⁶ Coleen K. Cunningham,⁷ Stephen A. Spector,⁸ Sharon Nachman,⁹ George K. Siberry,¹⁰ Edward Handelsman,^{11,†} Patricia M. Flynn¹² for IMPAACT P1088 study team

¹Department of Pediatrics; Division of Infectious Diseases; University of Colorado Denver; Aurora, CO USA; ²Frontier Science and Technology Research Foundation; Harvard School of Public Health; Boston, MA USA; ³Statistical and Data Analysis Center; Harvard School of Public Health; Boston, MA USA; ⁴Frontier Science and Technology Research Foundation; Amherst, NY USA; ⁵Social and Scientific Systems; International Maternal Pediatric Adolescent AIDS Clinical Trials Group; Durham, NC USA; ⁶Maternal; Child and Adolescent Virology Research Lab; University of South California; Los Angeles, CA USA; ⁷Duke University Medical Center; Duke Hospital; Durham, NC USA; ⁸Department of Pediatrics; Division of Infectious Diseases; University of California; San Diego, La Jolla, CA USA; ⁹Department of Pediatrics; State University of New York at Stony Brook; Stony Brook, NY USA; ¹⁰Pediatric Adolescent and Maternal AIDS Branch; Eunice Kennedy Shriver National Institute of Child Health and Human Development; National Institutes of Health; Bethesda, MD USA; ¹¹HIV Research Branch NIH; NIAID; DAIDS; TRP; Bethesda, MD USA; ¹²Department of Infectious Diseases; St. Jude Children's Research Hospital; Memphis, TN USA

[†]In memoriam

Keywords: HIV infection, influenza vaccine, cell-mediated immunity, regulatory T cells, regulatory B cells

Abbreviations: Breg, regulatory B cells; CDC, Centers for Disease Control; CMI, cell-mediated immunity; CTU, Clinical Trials Unit; ELISPOT, Enzyme-linked Immunosorbent Spot; GRB, granzyme B; HAART, highly active antiretroviral therapy; HAI, hemagglutination inhibition; HIV, human immunodeficiency virus; IMPAACT, International Maternal Pediatric and Adolescent Clinical Trials; IQR, interquartile range; LAIV, live-attenuated influenza vaccine; NIAID, National Institute of Allergy and Infectious Diseases; NICHD, National Institute of Child Health and Human Development; NIHM, National Institute of Mental Health; pH1N1, pandemic H1N1; TIV, trivalent inactivated vaccine; PACTG, Pediatric AIDS Clinical Trials Group; PBMC, peripheral blood mononuclear cells; PHA, phytohemagglutinin; SAS, statistical analysis system; SFC, spot forming cells; sH1N1, seasonal H1N1; TCID, tissue culture infective dose; Teff, effector T cells; Treg, regulatory T cells; VL, viral load

HIV-infected individuals have poor responses to inactivated influenza vaccines. To evaluate the potential role of regulatory T (Treg) and B cells (Breg), we analyzed their correlation with humoral and cell-mediated immune (CMI) responses to pandemic influenza (pH1N1) monovalent vaccine in HIV-infected children and youth. Seventy-four HIV-infected, 4- to 25-y old participants in a 2-dose pH1N1 vaccine study had circulating and pH1N1-stimulated Treg and Breg measured by flow cytometry at baseline, post-dose 1 and post-dose 2. Concomitantly, CMI was measured by ELISPOT and flow cytometry; and antibodies by hemagglutination inhibition (HAI). At baseline, most of the participants had pH1N1-specific IFN γ ELISPOT responses, whose magnitude positively correlated with the baseline pH1N1, but not with seasonal H1N1 HAI titers. pH1N1-specific IFN γ ELISPOT responses did not change post-dose 1 and significantly decreased post-dose 2. In contrast, circulating CD4+CD25+% and CD4+FOXP3+% Treg increased after vaccination. The decrease in IFN γ ELISPOT results was marginally associated with higher pH1N1-specific CD19+FOXP3+ and CD4+TGF β +% Breg and Treg, respectively. In contrast, increases in HAI titers post-dose 1 were associated with significantly higher circulating CD19+CD25+% post-dose 1, whereas increases in IFN γ ELISPOT results post-dose 1 were associated with higher circulating CD4+/C8+CD25+FOXP3+%. In conclusion, in HIV-infected children and youth, influenza-specific Treg and Breg may contribute to poor responses to vaccination. However, robust humoral and CMI responses to vaccination may result in increased circulating Treg and/or Breg, establishing a feed-back mechanism.

*Correspondence to: Adriana Weinberg; Email: adriana.weinberg@ucdenver.edu
Submitted: 09/17/12; Revised: 12/28/12; Accepted: 01/25/13
<http://dx.doi.org/10.4161/hv.23774>

Introduction

HIV-infected individuals generally mount poor responses to influenza vaccines.¹⁻⁵ In a study of the pandemic influenza (pH1N1) vaccine in HIV-infected children, adolescents and youth, P1088, we established that even after two doses with increased antigen content, antibody responses measured by hemagglutination inhibition (HAI) were lower than those described in age-matched historical controls receiving standard immunization regimens.⁶ In P1088, low HAI titers in response to pH1N1 vaccine correlated with low CD4 cell counts, which is in agreement with what has been typically found in vaccine studies in HIV-infected individuals, i.e., that advanced HIV disease, low CD4 cell counts and high plasma HIV viral loads (VL) are risk factors for decreased humoral or CMI responses to vaccines. However, the mechanism(s) responsible for the decreased immune responses to vaccines in the context of HIV infection is/are not known.

HIV-infected individuals have increased frequencies of regulatory T cells (Treg).⁷⁻⁹ Treg characteristically suppress CMI and can be identified by a series of markers, including high expression of CD25, FOXP3, IL10 and TGF β .¹⁰⁻¹² High Treg frequencies have been associated with the progression of HIV infection and with the development of opportunistic infections.^{7,13,14} The effect of Treg on responses to vaccines has not been extensively studied. Similarly, there is a dearth of information on the effect of regulatory B cells (Breg) on immune responses of HIV-infected individuals. Several subsets of Breg were identified in immune competent hosts and were characterized by high expression of the IL2 receptor CD25 and/or by production of the regulatory mediator IL10.^{15,16}

Protection against influenza infection is mediated both by antibodies and CMI.¹⁷⁻²¹ While neutralizing antibodies are able to prevent infection, CMI is particularly important in the clearance of infected cells.^{22,23} The live-attenuated influenza vaccine (LAIV), which confers superior protection against disease in children compared with the trivalent inactivated vaccine (TIV), generates robust CMI, but lower humoral responses than TIV,¹⁷ underscoring the importance of CMI in protection against influenza disease.

In this study, we describe the CMI, Treg and Breg responses of a cohort of HIV-infected children and youth and report the correlations of Treg and Breg frequencies with humoral and CMI responses to pH1N1.

Results

Demographic and other characteristics. Of the 74 P1088 subjects who contributed samples for this study, one was excluded because pH1N1 infection occurred before completing the full schedule of immunizations. The 73 remaining subjects were proportionally distributed across age groups (Table 1). The mean (S.D.) CD4%, CD8% and plasma HIV RNA at baseline were 34% (8.7%), 37% (12.9%) and 2.1 (0.8) log₁₀ copies/mL, respectively. Sixty-seven subjects (92%) were on HAART at enrollment. Approximately 26% of the subjects in each group

received seasonal influenza (sH1N1) vaccine \geq 2 weeks before the pH1N1 monovalent. The race, ethnicity and HIV disease characteristics were similar across age groups and between the subjects included in these advanced immunology analyses and the parent study subjects.

Kinetics of pH1N1-specific ELISPOT results in response to vaccination. After exclusion of samples with low viability or insufficient number of cells, 59 of 68 subjects with baseline data had positive IFN γ ELISPOT results for pH1N1 defined by \geq 50 spot forming cells (SFC)/10⁶ Peripheral blood mononuclear cells (PBMC). There were no significant differences in baseline IFN γ ELISPOT results by age at enrollment. pH1N1 IFN γ ELISPOT results remained unchanged from baseline to post-dose 1 with median [interquartile range (IQR)] of 317 (117, 673) and 363 (123, 622), respectively, but significantly decreased to 261 (78, 525) post-dose 2 ($p = 0.03$; Fig. 1A). Granzyme B (GrB) SFC at baseline had a median (IQR) of 35 (0, 220) and did not significantly change after vaccination (Fig. 1B). IFN γ or GrB ELISPOT responses to phytohemagglutinin (PHA) did not significantly change from baseline to post-dose 1 or 2 (Fig. 1C and D). Candida IFN γ ELISPOT responses tended to decrease between baseline and post-dose 2 ($p = 0.08$; Fig. 1E).

There was a positive correlation of the magnitude of baseline IFN γ ELISPOT results with the pH1N1 baseline HAI titers ($\rho = 0.29$; $p = 0.02$; Fig. 2A), but not with the sH1N1 baseline titers ($\rho = 0.04$; $p = 0.74$; not depicted). The association of pH1N1 IFN γ ELISPOT results with pH1N1 antibody titers continued post-dose 1 ($\rho = 0.25$, $p = 0.04$; Fig. 2B), but not post-dose 2 ($\rho = 0.01$; $p = 0.94$; Fig. 2C).

Baseline GrB ELISPOT responses to pH1N1 also correlated with baseline pH1N1 HAI titers ($\rho = 0.34$, $p = 0.01$; not depicted), but not with sH1N1 titers ($\rho = -0.03$, $p = 0.81$; not depicted). GrB ELISPOT responses post-dose 1 or 2 did not correlate with concomitant pH1N1 antibody titers (ρ of 0.08 and 0.07, respectively; p of 0.52 and 0.59, respectively; not depicted). GrB and IFN γ ELISPOT did not significantly correlate at baseline ($\rho = 0.19$, $p = 0.13$), but were correlated post-dose 1 and 2 ($\rho = 0.31$, $p = 0.01$ and $\rho = 0.40$, $p = 0.002$, respectively).

Kinetics of pH1N1-specific effector T cells (Teff) measured by flow cytometry. CD4⁺ and CD8⁺ Teff were characterized by IL2, TNF α , MIP1 β and perforin production after 48 h of in vitro stimulation with live pH1N1 or control. At baseline, median (IQR) influenza-specific CD4⁺IL2+%, CD4⁺MIP1 β %, CD4⁺perforin+%, CD4⁺TNF α +, CD8⁺IL2+%, CD8⁺MIP1 β %, CD8⁺perforin+%, and CD8⁺TNF α +, were 2.53 (1.52,4.12), 4.04 (2.57,7.38), 2.92 (1.35,5.29), 3.39 (2.04,6.70), 2.75 (1.60,5.35), 4.89 (2.50,7.33), 3.95 (2.65,7.08) and 3.42 (2.24,5.79). Corresponding numbers after the first dose of vaccine were 2.43 (1.28,3.92), 4.86 (2.11,9.10), 3.41 (1.98,5.75), 3.70 (2.20,6.83), 2.86 (1.36,5.29), 4.95 (2.12,8.21), 4.49 (2.58,7.17) and 3.38 (2.52,5.92); and after the second dose of vaccine 2.39 (1.51,4.37), 3.94 (1.95,6.59), 3.66 (1.80,5.45), 3.79 (1.87,6.42), 2.80 (1.64,4.22), 4.09 (2.05,7.84), 4.33 (2.40,6.80) and 3.67 (2.06,5.11). There were no significant changes in any of the Teff subsets after vaccination.

Kinetics of Treg and Breg subsets after pH1N1 vaccination. Circulating Treg and Breg were measured in freshly thawed unstimulated PBMC preparations and were characterized by FOXP3, CD25, IL10 and TGF β expression on CD4+, CD8+ and CD19+ lymphocytes. Significant increases were noted in CD4+CD25+% and CD4+FOXP3+% after the first dose of vaccine compared with baseline (p of 0.04 and 0.008, respectively; Fig. 3A and B). After the second dose of vaccine, CD4+CD25+% continued significantly higher than baseline, but CD4+FOXP3+% did not. All other circulating Treg and Breg subsets remained unchanged at all time points.

pH1N1-specific Treg and Breg were also measured after 48 h in vitro stimulation with pH1N1 virus and control. There were significant decreases in CD8+FOXP3+% and CD8+TGF β +% after the first dose of vaccine compared with baseline (p of 0.046 and 0.02, respectively; Fig. 4A and B), but not after the second dose of vaccine compared with baseline and not in other Treg or Breg subsets, including CD4+CD25+, CD4+FOXP3+, CD4+CD25+FOXP3+, CD4+TGF β +, CD4+IL10+, CD8+CD25+, CD8+CD25+FOXP3+, CD8+IL10+, CD19+CD25+, CD19+FOXP3+, CD19+CD25+FOXP3+ and CD19+IL10+.

Correlation analyses of HAI and ELISPOT responses with Treg and Breg subsets. To understand the potential role of Treg and Breg in modulating responses to vaccines in HIV-infected children and youth, we performed correlation analyses of the Treg and Breg subsets with changes in HAI titers and in IFN γ ELISPOT results. We found trend negative correlations between changes in IFN γ ELISPOT results from baseline to post-dose 1 and several pH1N1-stimulated Treg including CD19+FOXP3+% ($\rho = -0.25$, $p = 0.06$; Fig. 5A) and CD4+TGF β +% ($\rho = -0.22$, $p = 0.08$; Fig. 5B). In contrast, we found unexpected positive correlations of unstimulated CD19+CD25+% with the increase in pH1N1 log₁₀ HAI titers after the first dose of vaccine ($\rho = 0.27$, $p = 0.02$; Fig. 6A) and of CD4+CD25+FOXP3+% and CD8+CD25+FOXP3+% with IFN γ ELISPOT after the first dose of vaccine ($\rho = 0.24$, $p = 0.05$ and $\rho = 0.28$, $p = 0.03$, respectively; Fig. 6B and C).

Discussion

To our knowledge, this is the first study to systematically investigate Treg and Breg subsets after vaccination in a relatively large cohort of subjects ($n = 73$). We found an increase in circulating CD4+CD25+% and CD4+FOXP3+% after the first dose of vaccine. High expression of the CD25 IL2 receptor was one of the first described natural Treg characteristics. Natural Treg constitutively express CD25 in high abundance, which allows them to survive and proliferate in response to IL2 secretion.²⁴ However, activated Teff also upregulate their CD25 expression,²⁵ such that the CD4+CD25+ population may represent a mixture of circulating Treg and activated Teff. In contrast, the expression of FOXP3 is more specific for Treg, since it regulates Treg differentiation. Although FOXP3 may also be transiently expressed by activated T cells, the FOXP3+ Teff display lower cytokine production and proliferation compared with

Table 1. Demographics and HIV disease characteristics

	4–8 y of age	9–17 y of age	18–24 y of age	Total
Total number of subjects	24	23	26	73
Gender				
Female	14 (58%)	10 (43%)	14 (54%)	38 (52%)
Race and ethnicity				
Black	14 (58%)	14 (61%)	15 (58%)	43 (59%)
Latino	13 (54%)	10 (43%)	7 (27%)	30 (41%)
Age (yrs)				
Mean	6	13	20	13
Standard deviation	1.5	2	1.7	5.9
CD4 percent				
Mean	38	34	29	34
Standard deviation	6.9	6.4	10.2	8.7
CD8 percent				
Mean	28	38	44	37
Standard deviation	6.1	12.9	13	12.9
Log 10 RNA count				
Mean	1.8	1.8	2.5	2.1
Standard deviation	0.5	0.3	1.1	0.8

Notes: The lower limit of detection varied among subjects depending on the assay used at the specific clinical research site; RNA values below the limit of detection were replaced with the lower limit of the assay (e.g., 18 cp/mL was replaced with 50 cp/mL for an assay with the limit of detection of 50 cp/mL).

FOXP3- Teff and in some cases may evolve into Treg.^{26–28} Taken together, these data suggest that administration of pH1N1 vaccine to HIV-infected children and adolescents is associated with an increase of circulating activated and regulatory T cells.

Among the pH1N1-specific Treg subsets that we studied, we found decreases in CD8+TGF β +% and CD8+FOXP3+% after the first dose of vaccine. There were no increases in Th1 responses that might have explained the relative decrease of the proportions of pH1N1-specific CD8+ Treg. Other CD8+ T-cell subsets that were not measured in this study, such as those characterized by the production of IL4, IL5, IL13, IL9, IL22 or IL17, might have increased after vaccination, thus explaining the relative decrease of Treg.

This study confirmed our previous findings²⁹ that administration of influenza inactivated vaccines to HIV-infected children and youth was associated with a temporary decrease in Th1 CMI measured by IFN γ ELISPOT. In our previous study, we showed that HIV-infected children had a reduction of IFN γ ELISPOT responses to trivalent vaccine-homologous and heterologous influenza viruses and to phytohemagglutinin (PHA) at 28 d after vaccination. These responses, which were mostly derived from CD8+ cells, were partially recovered at 6 mo after vaccination.²⁹ Here, we extended these findings to pH1N1 monovalent inactivated vaccine. A large efficacy study would be necessary to determine the clinical implications of the relative CMI decrease after vaccination. Nevertheless, this identifies a CMI response to vaccination that seems to be specific to HIV-infected individuals,

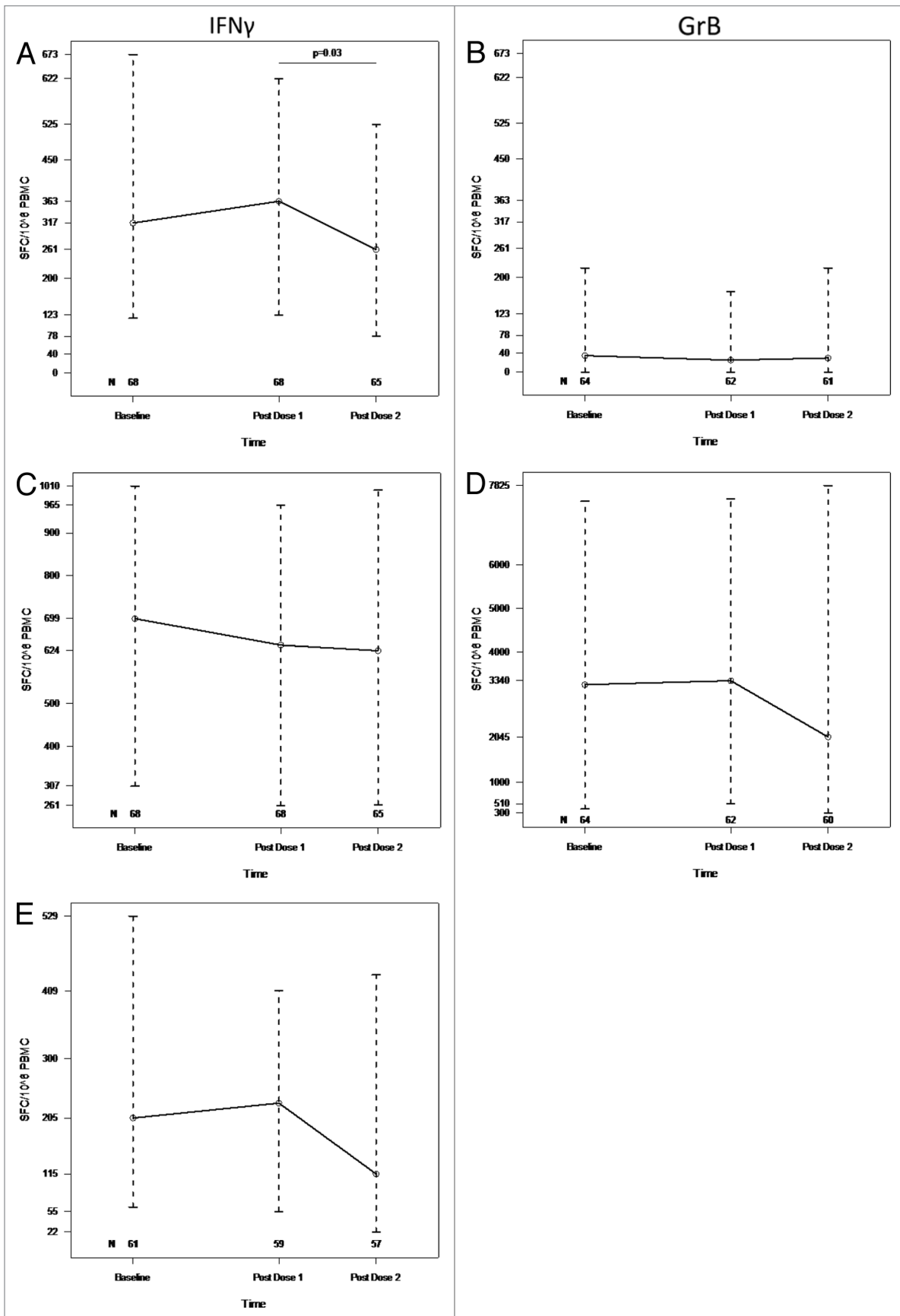


Figure 1. For figure legend, see page 961.

Figure 1 (See opposite page). pH1N1 IFN γ (A), GrB (B), PHA IFN γ (C), GrB (D) and Candida IFN γ (E) ELISPOT responses to two double-doses of pH1N1 vaccine. PBMC, frozen and thawed to preserve viability, were rested overnight. ELISPOT assays were performed only on PBMC with viability $\geq 70\%$ immediately after thawing and after resting. The assays used MabTech kits, live pH1N1 viral infection to promote stimulation of both CD4+ and CD8+ T cells, PHA mitogen and candida antigen controls. Results are presented as medians and IQRs. The number of subjects that contributed data at each time point are indicated on the graphs. Statistically significant differences assessed by Wilcoxon Matched Paired Signed Ranks test are shown on the graphs.

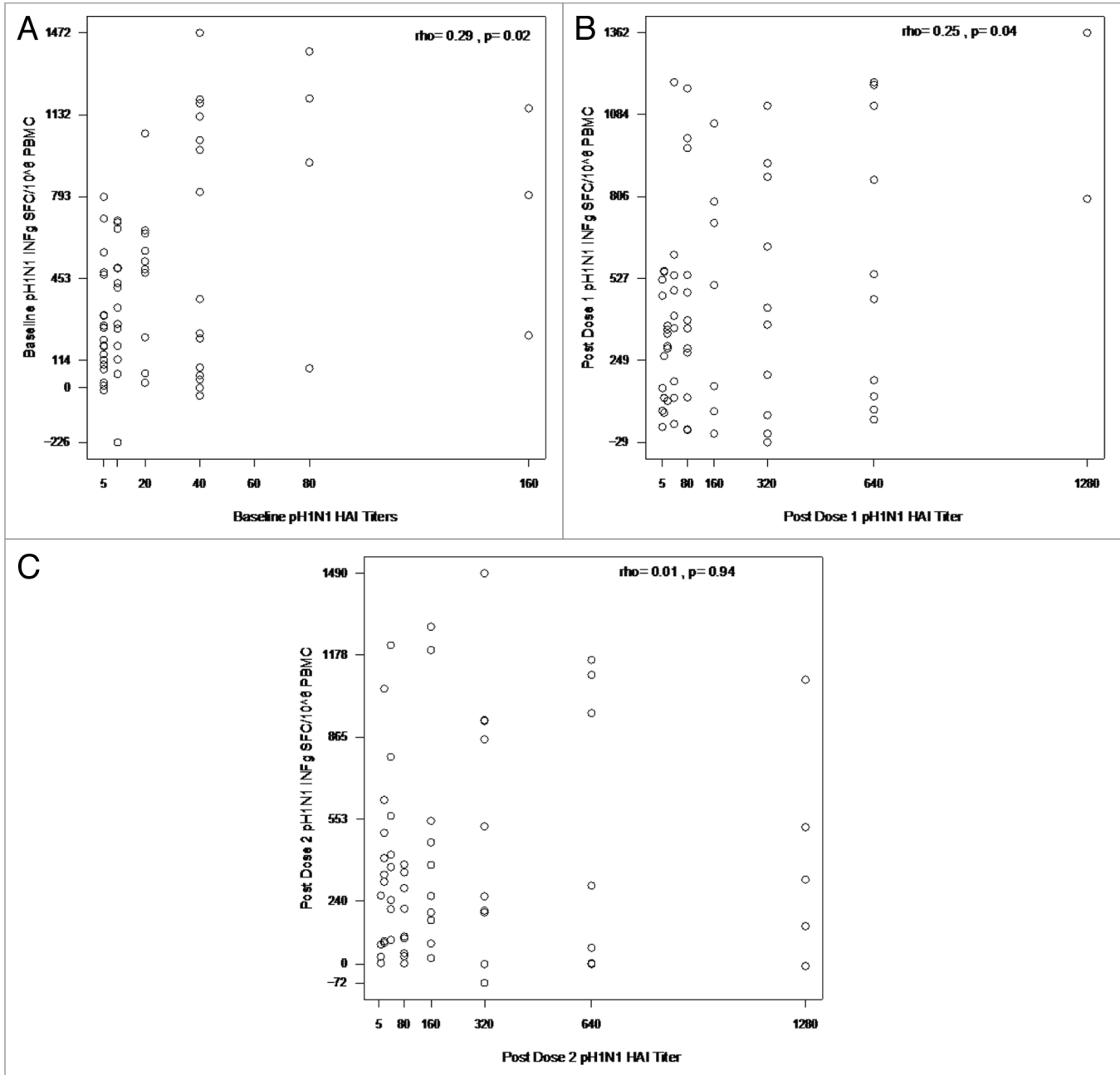


Figure 2. Correlations of pH1N1 IFN γ ELISPOT results with pH1N1 at baseline (A), post dose 1 (B) and post dose 2 (C). Data were derived from 67, 67 and 63 subjects in panels A, B and C, respectively. PBMC, frozen and thawed to preserve viability, were rested overnight. ELISPOT assays were performed only on PBMC with viability $\geq 70\%$ both immediately after thawing and after resting. The assays used MabTech kits and live pH1N1 viral infection to promote stimulation of both CD4+ and CD8+ T cells. HAI titers were measured using pH1N1 antigens. Assays are described in detail in the methods section. The coefficients of correlation and p values shown on each graph were calculated using Spearman correlation test.

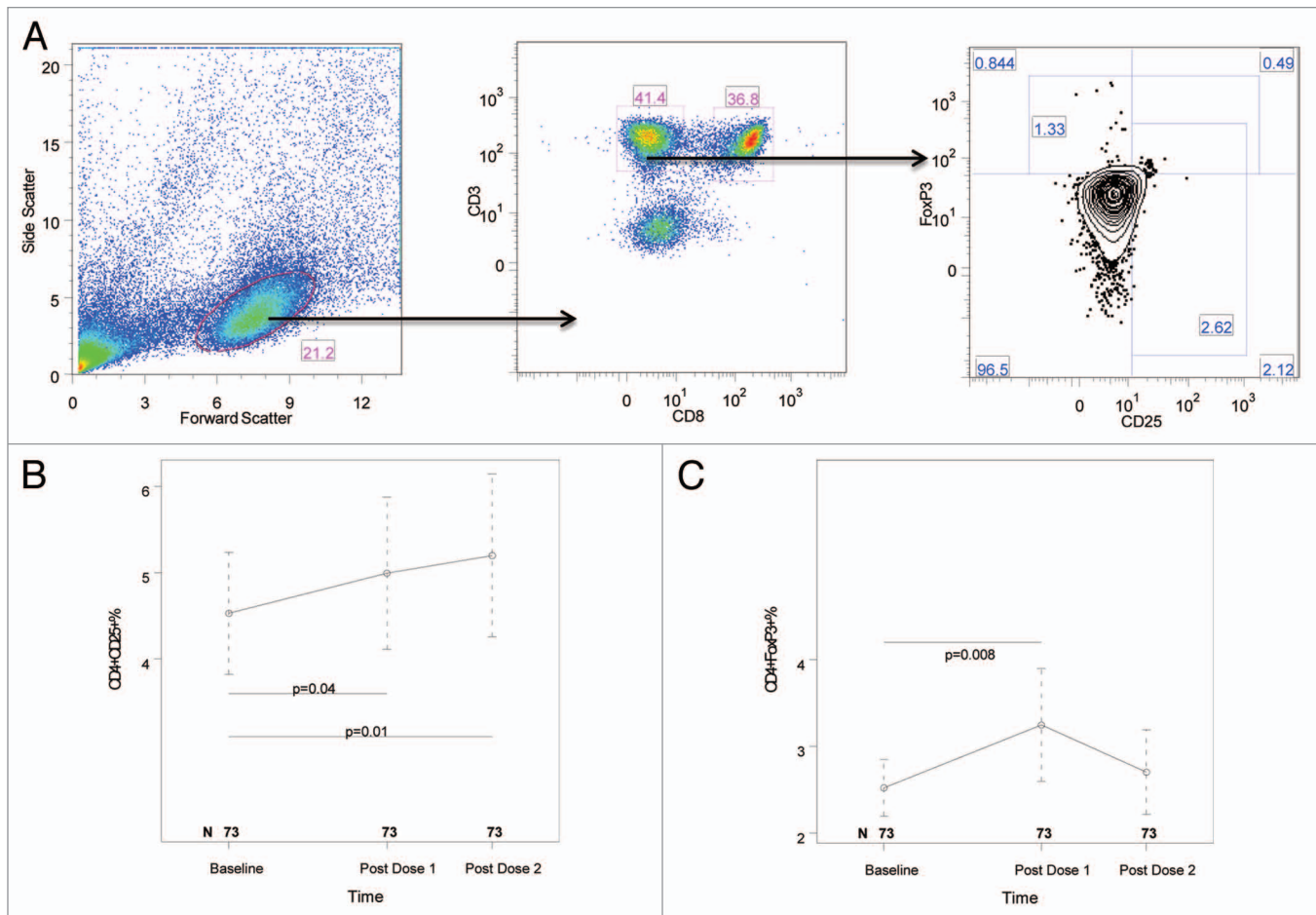


Figure 3. Kinetics of circulating CD4+CD25+ (B) and CD4+FOXP3+ (C) T cells after the two double-doses of pH1N1 vaccine. PBMC, frozen and thawed using procedures that preserve viability, were stained with mAbs anti-CD3, CD8, CD19, CD25 and FOXP3 and IL10 as described in the methods section. Panel A shows the gating strategy: (1) lymphocytes were identified by forward/side scatter; (2) CD4+ T cells were gated by expression of CD3 (CD3+) and lack of expression of CD8 (CD8-); (3) CD25+ and FOXP3+ CD4+ T cells were gated as shown. IL10 expression was gated using FOXP3 on one axis and IL10 on the other axis (not shown). CD8+ T cells were gated using expression of CD3 and CD8. B cells were gated as CD3-CD19+ (not shown). CD8+ T-cell and B-cell expression of CD25, FOXP3 and IL10 (not shown) were gated as described for CD4+ T cells. Panels B and C show only the lymphocyte subsets with significant changes over time. Results are presented as medians and IQRs. The number of subjects that contributed data at each time point are indicated on the graphs. Statistically significant differences assessed by Wilcoxon Matched Paired Signed Ranks test are shown on the graphs in panels B and C.

since it has not been observed in immunocompetent children or adults,^{30,31} and may be relevant to HIV immunopathogenesis.

To gain insight into the mechanism(s) that mediate the post-influenza vaccine CMI suppression, we investigated the association of IFN γ ELISPOT decreases after vaccination with pH1N1-specific Treg and Breg subsets. The loss in IFN γ ELISPOT responses after the first dose of the vaccine tended to occur in subjects with higher proportions of pH1N1-specific CD19+FOXP3+ and CD4+TGFB β + cells after the first dose of vaccine. This suggests that in HIV-infected vaccine recipients, increased proportions of pH1N1-specific Treg and Breg in response to vaccination may contribute to the attenuation of pH1N1-specific Teff responses to the vaccine. Since many of the participants were exposed to pH1N1 at baseline, the Treg response to pH1N1 stimulation may have resulted from previous exposure to the virus. Alternatively, exposure to seasonal H1N1, which has approximately 70% T-cell epitope homology

with pH1N1, may have accounted for the high proportion of pH1N1-specific Treg.

In contrast, subjects who gained pH1N1 IFN γ ELISPOT responses post-dose 1 compared with baseline also had increased proportions of circulating CD4+ and CD8+FOXP3+%. Furthermore, the increase in pH1N1 HAI titers post-dose 1 positively correlated with circulating CD19+CD25+%. As mentioned above, some of the CD4+ and CD8+FOXP3+ cells might represent transient expression of FOXP3 in Teff and conversion of Teff into Treg. Likewise, the CD19+CD25+ cells may represent a mixture of regulatory and activated B cells. Taken together, these data suggest that robust antigenic stimulation by the pH1N1 vaccine that increase the proportions of Teff also increase circulating Treg and Breg. This finding is consistent with data suggesting that activated conventional T cells generate Treg in the periphery.^{26,27} It also suggests that while T-cell activation is escalating, feed-back mechanisms meant to eventually quench the activation

are also initiated. Less is known about the genesis of Breg and further studies are needed in this area.

Influenza-specific GrB production was found to contribute significantly to protection against disease in elderly individuals.³²⁻³⁴ In this study, we found low frequencies of pH1N1-specific GrB-producing T cells even in baseline pH1N1-seropositive individuals who, presumably, developed pH1N1-specific GrB producing cells in response to wild-type infection. This is in accordance with previous observations that T cells of HIV-infected individuals have decreased production and secretion of GrB in response to antigenic stimulation.^{35,36} Furthermore, there were no significant increases in GrB ELISPOT results after vaccination.

We found significant correlations of pH1N1 IFN γ and GrB ELISPOT results with pH1N1 HAI titers at baseline. The specificity of this association was further underscored by the lack of correlation between pH1N1 IFN γ and GrB ELISPOT results with sH1N1 titers. This finding was not unexpected, since 30% of the study participants had evidence at baseline of undiagnosed, previous infection with pH1N1. Significant correlations of pH1N1 IFN γ with GrB ELISPOT responses were present post-dose 1 and 2, which was also expected considering that both assays measured Th1 type responses. There was also a significant correlation between pH1N1 IFN γ ELISPOT results and pH1N1 HAI titers after the first dose of vaccine. However, post-dose 2, there was a lack of correlation between pH1N1 IFN γ ELISPOT results, which decreased compared with baseline, and pH1N1 HAI titers, which increased compared with baseline.⁶ The post-dose 1 responses were primary responses in most subjects and the correlation of antibody and CMI could be viewed as evidence of the vaccine humoral and cellular immunogenicity. The post-dose 2 responses were anamnestic and show the dissociation between antibody and CMI anamnestic responses to influenza immunization in HIV-infected children and adolescents.

Our study was limited by the fact that enrollment started 6 mo into the pandemic, which resulted in a wild type infection rate of 30% at baseline. The rate of baseline seropositivity was within the range reported in other pH1N1 vaccine studies in HIV-infected individuals.³⁷⁻⁴⁰ Another potential limitation was the relatively homogeneous population with overall high CD4+ cell numbers and low HIV VL. However, in view of the recent recommendations to start antiretroviral therapy at progressively higher CD4+ cell numbers, we expect the immune status of our study population to constitute a good representation of the immune status of HIV-infected children and youth in the near future. Our study was also limited by the fact that only the blood compartment was investigated. We did not perform mean fluorescence intensity analyses and used a limited panel of Treg and Teff markers. However, this study included a large number of subjects compared with the majority of mechanistic studies. Thus, our results can be considered representative for the responses to pH1N1 vaccine in HIV-infected children and adolescents. This was a hypothesis-driven, novel investigation of the kinetics of Treg and Breg and their potential role in shaping responses to vaccines.

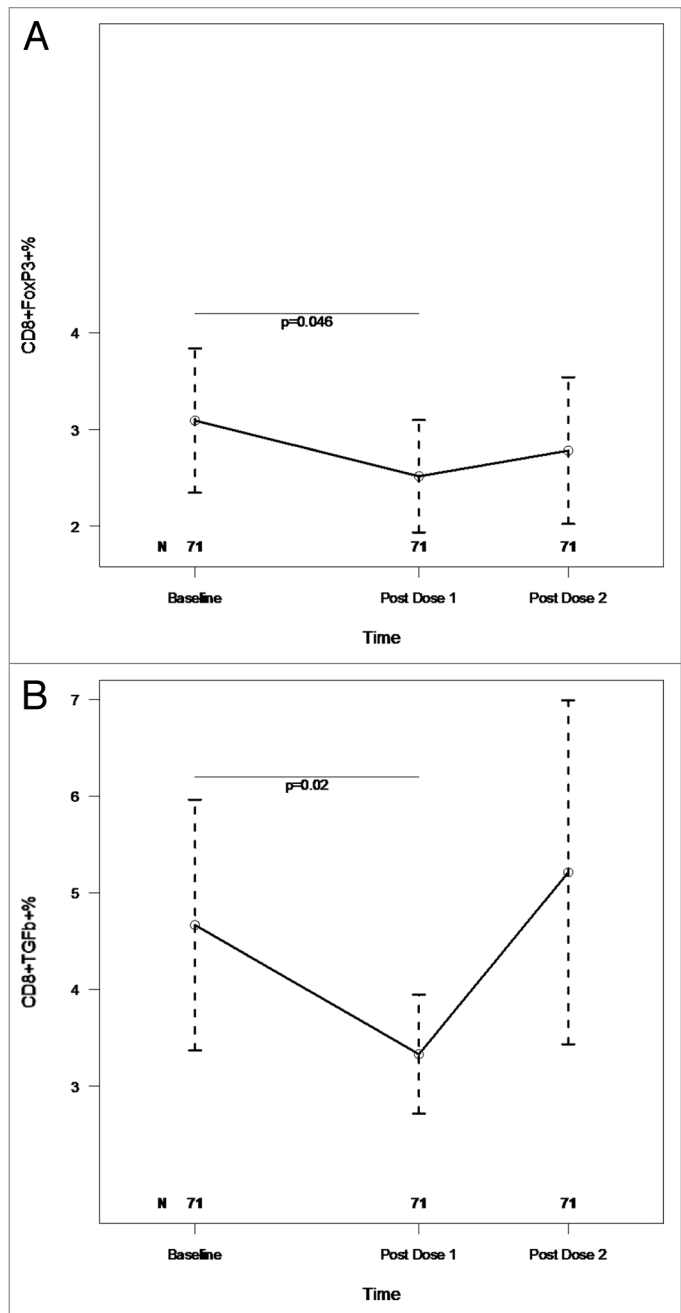


Figure 4. Kinetics of pH1N1-stimulated CD8+FOXP3+ (A) and CD8+TGFβ+ (B) T cells after the two double-doses of pH1N1 vaccine. PBMC with viability $\geq 70\%$ were incubated for 48 h with medium control and with live pH1N1 virus to promote stimulation through both MHC class I and class II. After incubation cells were stained with mAb anti-CD3, CD8, CD19, CD25, FOXP3 and IL10. Companion tubes were also stained with mAb anti-CD3, CD8, IL2, TNF α , MIP1 β and TGF β . The gating strategy (not shown) was similar to that described for freshly thawed, unstimulated PBMC (Fig. 3). The number of subjects that contributed data at each time point are indicated on the graphs. Results, depicted as medians and IQRs, are shown only for the lymphocyte populations with significant changes over time. Statistically significant differences assessed by Wilcoxon Matched Paired Signed Ranks test are shown on the graphs.

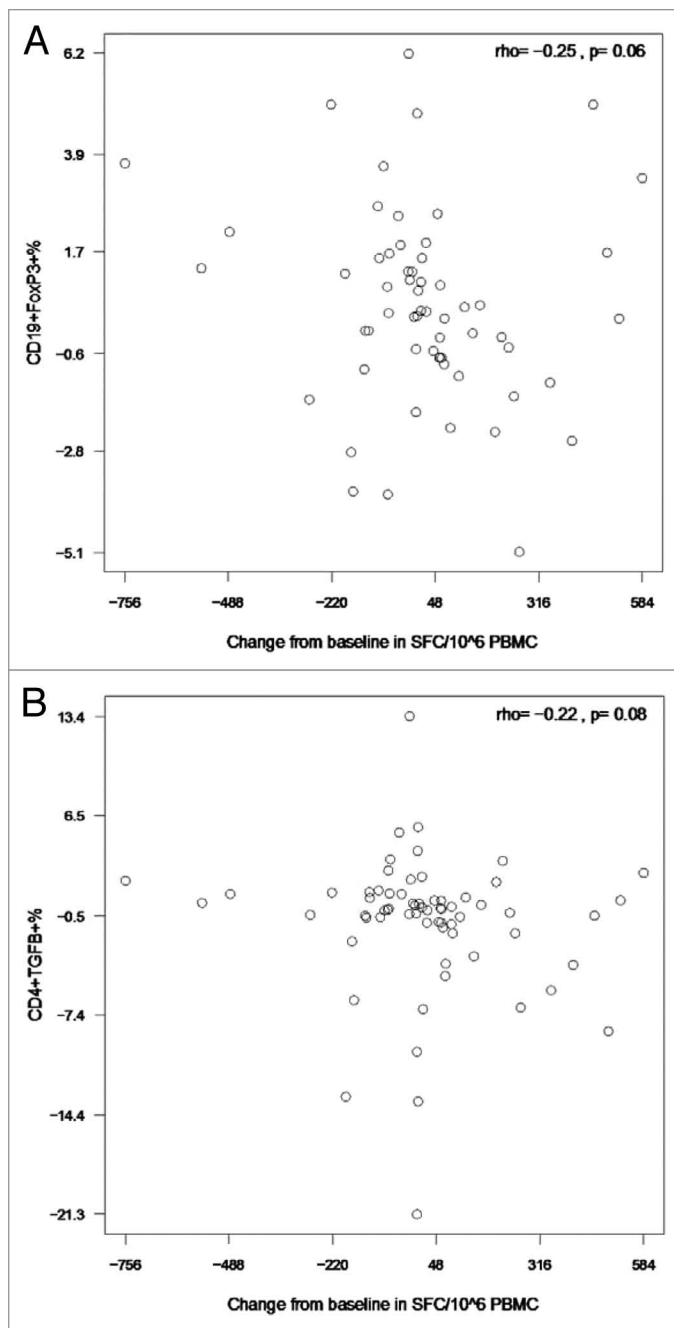


Figure 5. Correlations of pH1N1-stimulated IFN γ ELISPOT results after the first immunization with CD19+FOXP3+ % Breg (**A**) and CD4+TGF β + % Treg (**B**) after the first immunization. Data were derived from 63 and 66 participants in panels **A** and **B**, respectively. PBMC, frozen and thawed to preserve viability, were rested overnight. ELISPOT assays were performed only on PBMC with viability $\geq 70\%$ immediately after thawing and after resting. The assays used MabTech kits and live pH1N1 viral infection to promote stimulation of both CD4+ and CD8+ T cells. Flow cytometric assays were also performed on PBMC with viability $\geq 70\%$. Cells were incubated with pH1N1 live virus or medium control for 48 h after which they were stained as described in the methods section. The x axes represent the difference between baseline and post-dose 1 IFN γ ELISPOT results. The coefficients of correlation and p values shown on each graph were calculated using Spearman correlation test.

In conclusion, some Treg subsets increase in the circulation after influenza immunization of HIV-infected children and adolescents. These increases may occur in response to the antigenic stimulation provided by the immunogen, as they correlated with ELISPOT and HAI responses to the vaccine. pH1N1-specific Treg and Breg did not increase after vaccination. Nevertheless, higher pH1N1-specific Treg and Breg were associated with lower CMI responses to the vaccine. Further studies are warranted in other hosts that respond poorly to vaccines, such as transplant recipients and elderly individuals, to better understand the overall participation of regulatory mechanisms in responses to vaccines and to determine if Treg and Breg may be valuable targets for therapeutic interventions to improve immunogenicity of vaccines.

Methods and Materials

P1088 study design. Perinatally HIV-infected children and youth, aged ≥ 4 to < 25 y, were recruited from the International Maternal Pediatric and Adolescent Clinical Trials (IMPAACT) Network units in the US and Puerto Rico to participate in P1088. The study was approved by local IRBs. Legal guardians and/or subjects consented and/or assented to participate in this study. Subjects on stable ART for ≥ 90 d prior to entry received two 30 μg doses of 2009 Novartis Influenza A (pH1N1) monovalent vaccine (Fluvirin[®]) separated by 21–28 d. Seasonal influenza vaccine administration was restricted to ≥ 2 weeks before enrollment and to ≥ 2 weeks after the second pH1N1 dose. Blood for antibody and CMI assays was collected at baseline, 21–28 d post-dose 1 and 10–14 d post-dose 2. For this study, 74 participants with complete sets of PBMC, approximately equally distributed among the three age groups, were selected.

Antibody measurements. Sera were prepared at the clinical site laboratories, stored at $\leq -20^\circ\text{C}$ and shipped on dry ice or in liquid nitrogen containers to the testing laboratory at the University of Colorado Anschutz Medical Campus. pH1N1 and sH1N1 antibodies were measured by HAI assay using previously described methods¹ with a titer range of 1:10 to 1:1280. Sera with titers $< 1:10$ and $> 1:1280$ were arbitrarily ascribed values of 1:5 and 1:1280, respectively. Seroreponse was defined as having a ≥ 4 -fold rise in HAI titers following vaccination as compared with baseline HAI. A titer $\geq 1:40$ was considered protective.

IFN γ and GrB ELISPOT assays. PBMC were cryopreserved at the site laboratories according to a standardized protocol (<http://www.hanc.info/labs/Pages/SOPs.aspx>), stored at $\leq -150^\circ\text{C}$ and shipped in liquid nitrogen containers to the testing lab at University of Colorado Anschutz Medical Campus. Cells were thawed slowly as previously described.⁴¹ ELISPOT assays were performed using commercial ELISpot^{plus} kits (MabTech) as per manufacturer's instructions with modifications. To optimize detection of responses in HIV-infected individuals we used 500,000 PBMC per well. Thawed PBMC were allowed to sit overnight and resuspended at 10^6 PBMC/mL, in RPMI 1640 with glutamine (Gibco), 10% human AB serum (Gibco), 1% penicillin and streptomycin and 1% HEPES buffer. PBMC preparations with viability $\geq 70\%$, as measured by flow cytometry

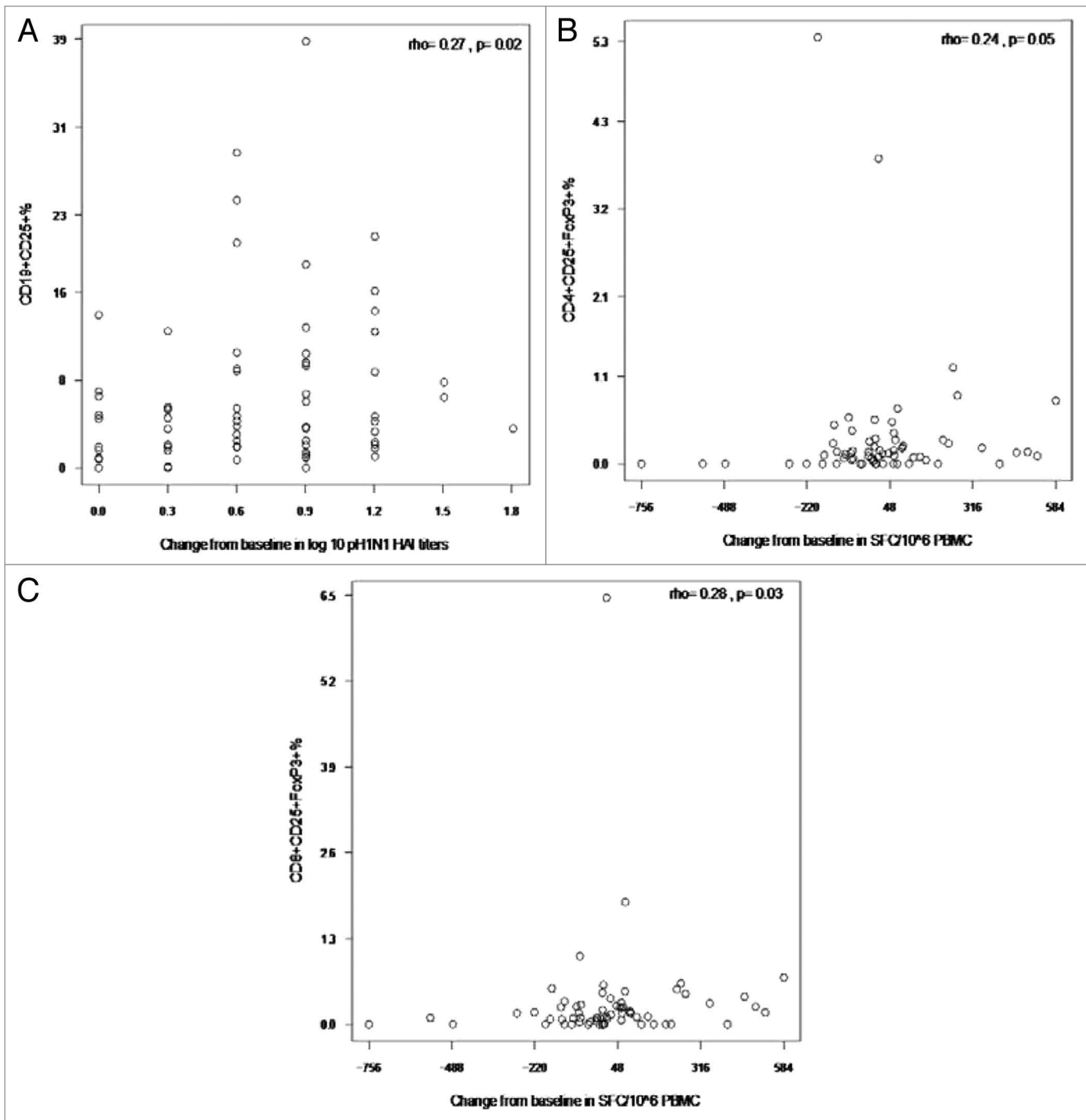


Figure 6. Correlations of pH1N1 antibody titers and of IFN γ ELISPOT results with circulating CD19+CD25+% B cells, CD4+CD25+FOXP3+% and CD8+CD25+FOXP3+% Treg after the first immunization. Data were derived from 72, 66 and 66 participants in panels **A–C**, respectively. The x axes represent the difference between baseline and post-dose 1 pH1N1 HAI (**A**) or IFN γ ELISPOT (**B and C**). HAI antibody titers to pH1N1 were measured as described in the methods section. PBMC, frozen and thawed to preserve viability, were rested overnight. ELISPOT assays were performed only on PBMC with viability $\geq 70\%$ both immediately after thawing and after resting. The assays used MabTech kits and live pH1N1 viral infection to promote stimulation of both CD4+ and CD8+ T cells. For flow cytometric analysis of circulating B and T cells, freshly thawed PBMC with adequate viability were stained with mAbs anti-CD3, CD8, CD19, CD25 and FOXP3 and IL10 as described in the methods section. The graphs depict only the correlations that reached statistical significance using the Spearman correlation test. Correlation coefficients and p values are shown on the graph.

using the Guava easyCyte 8HT instrument (Millipore), were used in these assays. Although viability $< 70\%$ may decrease the results of functional assays, assay results are stable and unaffected

by the viability $\geq 70\%$.⁴¹⁻⁴³ Cells were stimulated in duplicate wells with 2 TCID₅₀/PBMC of A/California/7/2009 Pandemic X-179A H1N1 Influenza virus (generous gift of Dr. A Klimov at

the CDC), 100 µg/mL candida antigen (Greer), 5 µg/mL phytohemagglutinin (PHA; Sigma) and unstimulated control. After a 48 h incubation at 37°C in a humidified 5% CO₂ atmosphere, plates were washed and stained with anti-IFN γ and anti-GrB mAbs as per manufacturer's instructions. SFC were revealed with colorimetric substrate and counted with an Immunospot S5 UV Analyzer (Cell Technologies Ltd). Results were expressed in SFC/10⁶ PBMC after subtracting the SFC in unstimulated control wells from those enumerated in antigen- or mitogen- stimulated wells.

Flow cytometry. Unstimulated Treg and Breg were measured in freshly thawed cryopreserved PBMC. After washing and counting viable cells, PBMC were surface-stained with the following conjugated mAbs: anti-CD3-PECy7 (BD Biosciences; BNI3), anti CD8-APC-AF 750 (Invitrogen; 3B5), anti-CD19-PECy5 (Invitrogen; SJ25-C1) and anti-CD25-APC (BD Biosciences; M-A251); then fixed and permeabilized with Cytotfix/Cytoperm (BD Biosciences) and stained with anti-IL-10-PE (BD Biosciences; JES3-19F1), anti-FOXP3-FITC (eBioscience; PCH101).

pH1N1-stimulated Treg, Breg and Teff were measured after pH1N1 in vitro stimulation. After overnight rest, PBMC resuspended at 10⁶ PBMC/mL in RPMI 1640 supplemented with antibiotics and 10% human AB serum were stimulated for 48 h with 2 TCID₅₀/cell of A/California/7/2009 Pandemic X-179A H1N1 Influenza virus or medium control in the presence of 1 µg/mL each anti-CD28 (BD Biosciences; L293) and anti-CD49d (BD Biosciences; B7651) mAbs. Brefeldin A (Sigma-Aldrich) was added to a final concentration of 10 µg/mL for the last 12–15 h of the incubation. Cells were stained using the following conjugated mAbs: anti-CD3-PECy7, anti-CD8-APC-AF 750, anti-CD19-PECy5, anti-IL-10-APC, anti-FOXP3-FITC, anti-TGF β -PE (Cederlane; TB21), anti-MIP1 β -PE (BD Biosciences; D21-1351), and anti-TNF α -PerCP Cy5.5 (Biolegend; MAb11), anti-Perforin-APC (Biolegend; dG9) and anti-IL2-FITC (BD Biosciences; 5344.111).

Total T and B cells and subpopulations were counted on Guava easyCyte 8HT (Millipore) and analyzed with FlowJo (Treestar). Subsets were expressed as a percentage of the parent CD3+CD4+, CD3+CD8+ or CD3-CD19+ cell population.

Statistical analyses. The baseline characteristics and safety data were summarized using descriptive measures. Changes in ELISPOT and flow cytometry-measured parameters between different time points were assessed using Wilcoxon Matched Pairs Signed Ranks and correlated t tests, respectively. The final analyses were restricted to flow cytometry samples with \geq 40 events in the anchor gate. However, a sensitivity analysis showed that the inclusion of samples with < 40 events in the anchor gate would not have changed the results. Spearman correlation analyses were performed to test associations. All analyses were performed using SAS Version 9.2 (SAS Institute INC) and the graphs were produced using the R software.

Disclosure of Potential Conflicts of Interest

This work was sponsored by the National Institute of Allergy and Infectious Diseases (NIAID) and The Eunice Kennedy Shriver

National Institute of Child Health and Human Development (NICHD).

Pharmaceutical support was provided by Novartis, through BARDA (Biomedical Advanced Research and Development Authority), Office of the Assistant Secretary for Preparedness and Response, US Department of Health and Human Services.

Acknowledgments

Members of the P1088 Protocol Team include: Patricia M. Flynn, MD, MS, St. Jude Children's Research Hospital, Memphis TN; Sharon Nachman, MD, SUNY Health Science Center at Stony Brook, Stony Brook, NY; Petronella Muresan, MS, Statistical and Data Analysis Center, Harvard School Public Health, Boston, MA; Terence Fenton, Ed D, Statistical and Data Analysis Center, Harvard School Public Health, Boston, MA; Stephen A. Spector, MD, University of California, San Diego, La Jolla, CA and Rady Children's Hospital; Coleen K. Cunningham, MD, Duke University Medical Center, Durham, NC; Robert Pass, MD, University of Alabama at Birmingham, Birmingham, AL; Ram Yogev, MD, Children's Memorial Hospital and Feinberg School of Medicine Northwestern University Medical School, Chicago, IL; Sandra Burchett, MD, MS, Children's Hospital Boston, Boston, MA; Barbara Heckman, BS, Frontier Science and Technology Research Foundation, Buffalo, NY; Anthony Bloom, BA, Frontier Science and Technology Research Foundation, Buffalo, NY; L. Jill Utech, RN, MSN, CCRC, St. Jude Children's Research Hospital, Memphis, TN; Patricia Anthony, BS, CLS, University of Southern California, Keck School of Medicine, Los Angeles, CA; Elizabeth Petzold, PhD, Social and Scientific Systems, Silver Spring, MD; Wende Levy, RN, MS, Social and Scientific Systems, Silver Spring, MD; Jennifer Bryant, MPA, Westat, Rockville, MD; George K. Siberry, MD, MPH, Pediatric Adolescent and Maternal AIDS Branch, Eunice Kennedy Shriver National Institute of Child Health and Development, Bethesda, MD; Ruth Ebiasah, Pharm D, MS, R Ph., Division of AIDS, National Institute of Allergy and Infectious Diseases, Bethesda, MD; Judi Miller, RN, BSN, Division of AIDS, National Institute of Allergy and Infectious Diseases, Bethesda, MD; Ed Handelsman, MD, Division of AIDS, National Institute of Allergy and Infectious Diseases, Bethesda, MD; Adriana Weinberg, MD, University of Colorado, Denver, Aurora, CO.

Participating sites and site personnel include: 60422 St. Jude/Memphis IMPAACT CTU (Nehali Patel, MD; Sandra Boyd, RN, MSN, PNP; Tom Wride, MS; Aditya Gaur, MD); 60402 The Children's Hospital of Philadelphia International Maternal Ped. Adolescent AIDS CTU (Steven D. Douglas, MD; Richard M. Rutstein, MD; Carol A. Vincent, CRNP, MSN; Margaret R. Duckett, RN, BSN); 60318 UCSD IMPAACT CTU (Rolando Viani, MD, MTP; Lisa Stangl, NP; Jeanne Manning, RN; Kimberly Norris, RN); 60336 Baylor College of Medicine CTU (Norma Cooper, MA, RN, BSN, ACRN; Mary Paul, MD; Kathleen Pitts, CPNP; Terry Raburn, RN); 60444 Bronx-Lebanon Hospital Family Ctr. CTU (Seema Chittalae, MD; Mavis Dummitt, RN; Stefan Hagmann, MD; Murli Purswani, MD); 5031 San Juan City Hospital PR NICHD CRS (Midnela Acevedo-Flores, MD; Wanda I. Marrero, BSN,

RN; Lizbeth Fabregas, BS,MS; Mario Paulino, MD); 5041 Children's Hospital of Michigan NICHD CRS (Chokechai Rongkavilit, MD; Ellen Moore, MD; Ulyssa Hancock, MSN, RN, PNP; Ayanna Walters, RN); 60325 Duke University Med. CTR. HIV/AIDS CTU (Joan Wilson; John Swetnam, M.Ed; Margaret Donnelly, PA-C, MS; Mary Jo Hassett, RN); 60341 Columbia Collaborative - HIV/AIDS CTU (Andrea Jurgau, MS, CPNP; Gina Silva, BSN; Seydi Vazquez Bonilla; Marc Foca, MD); 60358 NJ Med. School CRS (Arry Dieudonne, MD; Linda Bettica, RN; Juliette Johnson, RN; Lisa Monti, RN); 60466 UCLA-Los Angeles/Brazil AIDS Consortium (LABAC) CTU (Jaime Deville, MD; Karin Nielsen, MD; Nicole Falgout, RN; Yvonne Bryson, MD); 5045 Harbor UCLA Medical Center NICHD CRS (Margaret A. Keller, MD; Judy Hayes, RN; Yolanda Gonzalez, RN; Spring Wettgen, RN, PNP); 5052 University of Colorado Denver NICHD CRS (Emily Barr, CPNP, CNM, MSN; Jennifer Dunn, FNP-C; Suzanne Paul, FNP-C; Carol Salbenblatt, RN, MSN; CCTSI Grant: UL1 TR000154); 5055 South Florida CDC Ft Lauderdale NICHD CRS (Ana Puga, MD; Kathleen Graham, Pharm D; Zulma Eysallenne, RN; Dayana Leon); 5083 Rush University Cook County Hospital Chicago NICHD CRS (Maureen McNichols, RN, MSN; Elizabeth Jones, RN, MSN; James B. McAuley, MD, MPH); 5093 Miller Children's Hospital Long Beach CA (Audra Deveikis, MD; Tempe K. Chen, MD; David E. Michalik, DO; Jagmohan Batra, MD); 5094 University of Maryland Baltimore NICHD CRS; 60323 WNE Maternal Pediatric Adolescent AIDS CTU (Katherine Luzuriaga, MD; Jessica Pagano-Therrien, RN, NP; CTSA Grant: UL1RR031982); 60349 University of Miami PED. Perinatal HIV/AIDS CTU (Gwendolyn B. Scott, MD; Charles D. Mitchell, MD; Patricia Bryant, RN, BSN; Claudia Florez, MD); 5013 Jacobi Med. CTR. Bronx NICHD CRS (Joanna Dobroszycki, MD; Marlene Burey, RN, MSHS, CPN; Raphaelle Auguste, RN, BSN; Karen Kassen, RN); 5017 Seattle Children's Hospital CRS (Ann J Melvin, MD, MPH; Joycelyn Thomas, RN; Corry Venema-Weiss, ARNP; Lisa M Frenkel, MD); 5040 Suny Stony Brook NICHD CRS (Denise Ferraro FNP; Michele Kelly, NP; Erin Infanzon); 60339 Children's Memorial Hospital - Chicago (Ellen Chadwick, MD; Jennifer Jensen, PNP; Lynn Heald, PNP; Ruth Williams, RN); 5048 University of Southern California LA (James Homans, MD, MPH; Andrea Kovacs, MD; LaShonda Spencer, MD; Michael Neely, MD, MSc, FCP); 5051 University of Florida College of Medicine, Jacksonville (Mobeen Rathore, MD; Ayesha Mirza, MD; Nizar Maraqa, MD; Kathleen A. Thoma, MA, CCRP; CCTSI Grant: UL1 RR029890); 5057

Strong Memorial Hospital, University of Rochester (Geoffrey A. Weinberg, MD; Barbra Murante, MS, RN, PNP); 5091 University of California San Francisco NICHD CRS (Diane W. Wara, MD; Mica Muscat, PNP; Nicole Tilton, PNP; Ted Ruel, MD); 5096 University of Alabama Birmingham NICHD CRS (Marilyn Crain, MPH, MD; Tina Simpson, MD, MPH; Sharan Robbins, BA; Dorothy Shaw, BA); 60446 University of Puerto Rico CTU (Carmen D. Zorrilla, MD; Irma Febo, MD; Vivian Tamayo-Agrait, MD; Ruth Santos- Otero, RN); 5015 Children's National Med. CTR. Washington DC NICHD CRS (Steven Zeichner, MD, PhD; Deidre Thompson, RN; Chrisa Thomas, BA); 5018 USF - Tampa NICHD CRS (Jorge Lujan-Zilberman, MD; Patricia Emmanuel, MD; Denise Casey, RN; Tammy Myers); 5009 Children's Hospital of Boston NICHD CRS (Sandra K. Burchett, MD, MSc; Nancy Karthas, RN, MS, CPNP; Catherine Kneut, RN, MS, CPNP; Lisa Tucker, BFA); 5044 Howard University Washington DC NICHD CRS (Sohail Rana, MD; Meseret Deressa, MD, MPH; Helga Finke, MD; Patricia Houston, MS); 5012 NYU NY NICHD CRS (Sandra Deygoo, MS; Siham Akleh, RN; Aditya Kaul, MD; William Borkowsky, MD; CCTSI Grant: 1UL1RR029893); 5003 Metropolitan Hospital NICHD CRS (Mahrukh Bamji MD; Santa Paul, MD; Siobhan Riley, MPH); 5092 Johns Hopkins University, Baltimore (Allison Agwu, MD, ScM; Todd Noletto, MPH; Jennifer Chang, BS; Andi Weiss, RPH); 5011 Boston Medical Center PED. HIV Program NICHD CRS (Ellen R. Cooper, MD; Debra McLaud, RN; Diana Clarke, Pharm D; CCTSI Grant: U54 RR025771).

Overall support for the International Maternal Pediatric Adolescent AIDS Clinical Trials Group (IMPAACT) was provided by the National Institute of Allergy and Infectious Diseases (NIAID) [U01 AI068632], the Eunice Kennedy Shriver National Institute of Child Health and Human Development (NICHD) and the National Institute of Mental Health (NIMH) [AI068632]. The content is solely the responsibility of the authors and does not necessarily represent the official views of the NIH. This work was supported by the Statistical and Data Analysis Center at Harvard School of Public Health, under the National Institute of Allergy and Infectious Diseases cooperative agreement #5 U01 AI41110 with the Pediatric AIDS Clinical Trials Group (PACTG) and #1 U01 AI068616 with the IMPAACT Group. Support of the sites was provided by the National Institute of Allergy and Infectious Diseases (NIAID) and the NICHD International and Domestic Pediatric and Maternal HIV Clinical Trials Network funded by NICHD (contract number N01-DK-9-001/HHSN267200800001C).

References

1. Levin MJ, Song LY, Fenton T, Nachman S, Patterson J, Walker R, et al. Shedding of live vaccine virus, comparative safety, and influenza-specific antibody responses after administration of live attenuated and inactivated trivalent influenza vaccines to HIV-infected children. *Vaccine* 2008; 26:4210-7; PMID:18597900; <http://dx.doi.org/10.1016/j.vaccine.2008.05.054>.
2. Malaspina A, Moir S, Orsega SM, Vasquez J, Miller NJ, Donoghue ET, et al. Compromised B cell responses to influenza vaccination in HIV-infected individuals. *J Infect Dis* 2005; 191:1442-50; PMID:15809902; <http://dx.doi.org/10.1086/429298>.
3. Cooper C, Thorne A, Klein M, Conway B, Boivin G, Haase D, et al.; CIHR Canadian HIV Trials Network Influenza Vaccine Research Group. Immunogenicity is not improved by increased antigen dose or booster dosing of seasonal influenza vaccine in a randomized trial of HIV infected adults. *PLoS One* 2011; 6:e17758; PMID:21512577; <http://dx.doi.org/10.1371/journal.pone.0017758>.
4. Crum-Cianflone NF, Eberly LE, Duplessis C, Maguire J, Ganesan A, Faix D, et al. Immunogenicity of a monovalent 2009 influenza A (H1N1) vaccine in an immunocompromised population: a prospective study comparing HIV-infected adults with HIV-uninfected adults. *Clin Infect Dis* 2011; 52:138-46; PMID:21148532; <http://dx.doi.org/10.1093/cid/ciq019>.
5. Kosalaraksa P, Srirompotong U, Newman RW, Lumbiganon P, Wood JM. Serological response to trivalent inactivated influenza vaccine in HIV-infected children with different immunologic status. *Vaccine* 2011; 29:3055-60; PMID:21349365; <http://dx.doi.org/10.1016/j.vaccine.2011.01.091>.

6. Flynn PM, Nachman S, Muresan P, Fenton T, Spector SA, Cunningham CK, et al.; IMPAACT P1088 Team. Safety and immunogenicity of 2009 pandemic H1N1 influenza vaccination in perinatally HIV-1-infected children, adolescents, and young adults. *J Infect Dis* 2012; 206:421-30; PMID:22615311; <http://dx.doi.org/10.1093/infdis/jis360>.
7. Presicce P, Orsborn K, King E, Pratt J, Fichtenbaum CJ, Chougnet CA. Frequency of circulating regulatory T cells increases during chronic HIV infection and is largely controlled by highly active antiretroviral therapy. [Electronic Resource]. *PLoS One* 2011; 6:e28118; PMID:22162758; <http://dx.doi.org/10.1371/journal.pone.0028118>.
8. Hunt PW, Landay AL, Sinclair E, Martinson JA, Hatano H, Emu B, et al. A low T regulatory cell response may contribute to both viral control and generalized immune activation in HIV controllers. *PLoS One* 2011; 6:e15924; PMID:21305005; <http://dx.doi.org/10.1371/journal.pone.0015924>.
9. Lim A, Tan D, Price P, Kamarulzaman A, Tan HY, James I, et al. Proportions of circulating T cells with a regulatory cell phenotype increase with HIV-associated immune activation and remain high on antiretroviral therapy. *AIDS* 2007; 21:1525-34; PMID:17630546; <http://dx.doi.org/10.1097/QAD.0b013e32825cab8b>.
10. Allan SE, Passerini L, Bacchetta R, Crellin N, Dai M, Urban PC, et al. The role of 2 FOXP3 isoforms in the generation of human CD4+ Tregs. *J Clin Invest* 2005; 115:3276-84; PMID:16211090; <http://dx.doi.org/10.1172/JCI24685>.
11. Walker MR, Carson BD, Nepom GT, Ziegler SF, Buckner JH. De novo generation of antigen-specific CD4+CD25+ regulatory T cells from human CD4+CD25- cells. *Proc Natl Acad Sci U S A* 2005; 102:4103-8; PMID:15753318; <http://dx.doi.org/10.1073/pnas.0407691102>.
12. Jonuleit H, Schmitt E. The regulatory T cell family: distinct subsets and their interrelations. *J Immunol* 2003; 171:6323-7; PMID:14662827.
13. Andersson J, Boasso A, Nilsson J, Zhang R, Shire NJ, Lindback S, et al. The prevalence of regulatory T cells in lymphoid tissue is correlated with viral load in HIV-infected patients. *J Immunol* 2005; 174:3143-7; PMID:15749840.
14. Moreno-Fernandez ME, Rueda CM, Velilla PA, Rugeles MT, Chougnet CA. cAMP during HIV infection: friend or foe? *AIDS Res Hum Retroviruses* 2012; 28:49-53; PMID:21916808; <http://dx.doi.org/10.1089/aid.2011.0265>.
15. Iwata Y, Matsushita T, Horikawa M, Dilillo DJ, Yanaba K, Venturi GM, et al. Characterization of a rare IL-10-competent B-cell subset in humans that parallels mouse regulatory B10 cells. *Blood* 2011; 117:530-41; PMID:20962324; <http://dx.doi.org/10.1182/blood-2010-07-294249>.
16. Tretter T, Venigalla RK, Eckstein V, Saffrich R, Sertel S, Ho AD, et al. Induction of CD4+ T-cell anergy and apoptosis by activated human B cells. *Blood* 2008; 112:4555-64; PMID:18802006; <http://dx.doi.org/10.1182/blood-2008-02-140087>.
17. Forrest BD, Pride MW, Dunning AJ, Capeding MR, Chotpitayasunondh T, Tam JS, et al. Correlation of cellular immune responses with protection against culture-confirmed influenza virus in young children. *Clin Vaccine Immunol* 2008; 15:1042-53; PMID:18448618; <http://dx.doi.org/10.1128/CVI.00397-07>.
18. Ohmit SE, Petrie JG, Cross RT, Johnson E, Monto AS. Influenza hemagglutination-inhibition antibody titer as a correlate of vaccine-induced protection. *J Infect Dis* 2011; 204:1879-85; PMID:21998477; <http://dx.doi.org/10.1093/infdis/jir661>.
19. Hara M, Tanaka K, Kase T, Maeda A, Hirota Y. Evaluation of seasonal influenza vaccination effectiveness based on antibody efficacy among the institutionalized elderly in Japan. *Vaccine* 2010; 28:5664-8; PMID:20600482; <http://dx.doi.org/10.1016/j.vaccine.2010.06.061>.
20. Black S, Nicolay U, Vesikari T, Knuff M, Del Giudice G, Della Cioppa G, et al. Hemagglutination inhibition antibody titers as a correlate of protection for inactivated influenza vaccines in children. *Pediatr Infect Dis J* 2011; 30:1081-5; PMID:21983214; <http://dx.doi.org/10.1097/INF.0b013e3182367662>.
21. Belshe RB, Gruber WC, Mendelman PM, Mehta HB, Mahmood K, Reisinger K, et al. Correlates of immune protection induced by live, attenuated, cold-adapted, trivalent, intranasal influenza virus vaccine. *J Infect Dis* 2000; 181:1133-7; PMID:10720541; <http://dx.doi.org/10.1086/315323>.
22. Thomas PG, Keating R, Hulse-Post DJ, Doherty PC. Cell-mediated protection in influenza infection. *Emerg Infect Dis* 2006; 12:48-54; PMID:16494717; <http://dx.doi.org/10.3201/eid1201.051237>.
23. Mbawuike IN, Zhang Y, Couch RB. Control of mucosal virus infection by influenza nucleoprotein-specific CD8+ cytotoxic T lymphocytes. *Respir Res* 2007; 8:44; PMID:17597533; <http://dx.doi.org/10.1186/1465-9921-8-44>.
24. Xia G, He J, Zhang Z, Leventhal JR. Targeting acute allograft rejection by immunotherapy with ex vivo-expanded natural CD4+ CD25+ regulatory T cells. *Transplantation* 2006; 82:1749-55; PMID:17198271; <http://dx.doi.org/10.1097/01.tp.0000250731.44913.ee>.
25. Raimondi G, Shufesky WJ, Tokita D, Morelli AE, Thomson AW. Regulated compartmentalization of programmed cell death-1 discriminates CD4+CD25+ resting regulatory T cells from activated T cells. *J Immunol* 2006; 176:2808-16; PMID:16493037.
26. McMurchy AN, Gillies J, Gizzi MC, Riba M, Garcia-Manteiga JM, Cittaro D, et al. A novel function for FOXP3 in humans: intrinsic regulation of conventional T cells. *Blood* 2012; In Press; PMID:23169781; <http://dx.doi.org/10.1182/blood-2012-05-431023>.
27. Walker MR, Kasprovicz DJ, Gersuk VH, Benard A, Van Landeghen M, Buckner JH, et al. Induction of FoxP3 and acquisition of T regulatory activity by stimulated human CD4+CD25- T cells. *J Clin Invest* 2003; 112:1437-43; PMID:14597769.
28. Vukmanovic-Stejic M, Zhang Y, Cook JE, Fletcher JM, McQuaid A, Masters JE, et al. Human CD4+ CD25hi Foxp3+ regulatory T cells are derived by rapid turnover of memory populations in vivo. *J Clin Invest* 2006; 116:2423-33; PMID:16955142; <http://dx.doi.org/10.1172/JCI28941>.
29. Weinberg A, Song LY, Fenton T, Nachman SA, Read JS, Patterson-Bartlett J, et al. T cell responses of HIV-infected children after administration of inactivated or live attenuated influenza vaccines. *AIDS Res Hum Retroviruses* 2010; 26:51-9; PMID:20059397; <http://dx.doi.org/10.1089/aid.2009.0163>.
30. Hammit LL, Bartlett JP, Li S, Rahkola J, Lang N, Janoff EN, et al. Kinetics of viral shedding and immune responses in adults following administration of cold-adapted influenza vaccine. *Vaccine* 2009; 27:7359-66; PMID:19800447; <http://dx.doi.org/10.1016/j.vaccine.2009.09.041>.
31. He XS, Holmes TH, Zhang C, Mahmood K, Kemble GW, Lewis DB, et al. Cellular immune responses in children and adults receiving inactivated or live attenuated influenza vaccines. *J Virol* 2006; 80:11756-66; PMID:16971435; <http://dx.doi.org/10.1128/JVI.01460-06>.
32. McElhaney JE, Ewen C, Zhou X, Kane KP, Xie D, Hager WD, et al. Granzyme B: Correlates with protection and enhanced CTL response to influenza vaccination in older adults. *Vaccine* 2009; 27:2418-25; PMID:19368783; <http://dx.doi.org/10.1016/j.vaccine.2009.01.136>.
33. McElhaney JE, Gravenstein S, Upshaw CM, Hooton JW, Krause P, Drinka P, et al. Granzyme B: a marker of risk for influenza in institutionalized older adults. *Vaccine* 2001; 19:3744-51; PMID:11395209; [http://dx.doi.org/10.1016/S0264-410X\(01\)00087-1](http://dx.doi.org/10.1016/S0264-410X(01)00087-1).
34. McElhaney JE, Pinkoski MJ, Upshaw CM, Bleackley RC. The cell-mediated cytotoxic response to influenza vaccination using an assay for granzyme B activity. *J Immunol Methods* 1996; 190:11-20; PMID:8601703; [http://dx.doi.org/10.1016/0022-1759\(95\)00235-9](http://dx.doi.org/10.1016/0022-1759(95)00235-9).
35. Yang OO, Lin H, Dagarag M, Ng HL, Effros RB, Uittenbogaart CH. Decreased perforin and granzyme B expression in senescent HIV-1-specific cytotoxic T lymphocytes. *Virology* 2005; 332:16-9; PMID:15661136; <http://dx.doi.org/10.1016/j.virol.2004.11.028>.
36. Bosch Princep R, Lejeune M, Salvadó Usach MT, Jaén Martínez J, Pons Ferré LE, Alvaro Naranjo T. Decreased number of granzyme B+ activated CD8+ cytotoxic T lymphocytes in the inflammatory background of HIV-associated Hodgkin's lymphoma. *Ann Hematol* 2005; 84:661-6; PMID:15875183; <http://dx.doi.org/10.1007/s00277-005-1051-3>.
37. Lagler H, Grabmeier-Pfistershammer K, Touzeau-Römer V, Tobudic S, Ramharter M, Wenisch J, et al. Immunogenicity and tolerability after two doses of non-adjuncted, whole-virion pandemic influenza A (H1N1) vaccine in HIV-infected individuals. *PLoS One* 2012; 7:e36773; PMID:22629330; <http://dx.doi.org/10.1371/journal.pone.0036773>.
38. Phongsamart W, Sirisanthana V, Wittawatmongkol O, Malesatharn A, Sudjaritruk T, Chearskul P, et al. Immunogenicity and safety of monovalent influenza A (H1N1) 2009 in HIV-infected Thai children. *Vaccine* 2011; 29:8705-11; PMID:21893147; <http://dx.doi.org/10.1016/j.vaccine.2011.08.101>.
39. Maruszak H, Jeganathan S, Smith DE, Robertson P, Barnes T, Furner V. Improved serological response to H1N1 monovalent vaccine associated with viral suppression among HIV-1-infected patients during the 2009 influenza (H1N1) pandemic in the Southern Hemisphere. *HIV Med* 2012; 13:352-7; PMID:22296264; <http://dx.doi.org/10.1111/j.1468-1293.2011.00987.x>.
40. Tebas P, Frank I, Lewis M, Quinn J, Zifchak L, Thomas A, et al.; Center for AIDS Research and Clinical Trials Unit of the University of Pennsylvania. Poor immunogenicity of the H1N1 2009 vaccine in well controlled HIV-infected individuals. *AIDS* 2010; 24:2187-92; PMID:20616698; <http://dx.doi.org/10.1097/QAD.0b013e32833c6d5c>.
41. Weinberg A, Song LY, Wilkening CL, Fenton T, Hural J, Louzao R, et al. Optimization of storage and shipment of cryopreserved peripheral blood mononuclear cells from HIV-infected and uninfected individuals for ELISPOT assays. *J Immunol Methods* 2010; 363:42-50; PMID:20888337; <http://dx.doi.org/10.1016/j.jim.2010.09.032>.
42. Weinberg A, Song LY, Wilkening C, Sevin A, Blais B, Louzao R, et al.; Pediatric ACTG Cryopreservation Working Group. Optimization and limitations of use of cryopreserved peripheral blood mononuclear cells for functional and phenotypic T-cell characterization. *Clin Vaccine Immunol* 2009; 16:1176-86; PMID:19515870; <http://dx.doi.org/10.1128/CVI.00342-08>.
43. Bull M, Lee D, Stucky J, Chiu YL, Rubin A, Horton H, et al. Defining blood processing parameters for optimal detection of cryopreserved antigen-specific responses for HIV vaccine trials. *J Immunol Methods* 2007; 322:57-69; PMID:17382342; <http://dx.doi.org/10.1016/j.jim.2007.02.003>.